Ultrastructural and Spectrophotometric Study on the Effects of Putative Triggers on Aortic Valve Interstitial Cells in *In Vitro* Models Simulating Metastatic Calcification

ANTONELLA BONETTI,[1] ALBERTO DELLA MORA,[1] MAGALI CONTIN,[1] FRANCO TUBARO,[2] MAURIZIO MARCHINI,[1] AND FULVIA ORTOLANI[1]*

[1]Department of Experimental Clinical Medicine, University of Udine, Piazzale Kolbe 3, Udine, Italy

[2]Department of Food Sciences, University of Udine, Via delle Scienze 208, Udine, Italy

ABSTRACT

Metastatic calcification of cardiac valves is a common complication in patients affected by chronic renal failure. In this study, primary bovine aortic valve interstitial cells (AVICs) were subjected to pro-calcific treatments consisting in cell stimulation with (i) elevated inorganic phosphate (Pi = 3 mM), to simulate hyperphosphatemic conditions; (ii) bacterial endotoxin lipopolysaccharide (LPS), simulating direct effects by microbial agents; and (iii) conditioned media (CM) derived from cultures of either LPS-stimulated heterogenic macrophages (commercial murine RAW264.7 cells) or LPS-stimulated fresh allogenic monocytes/macrophages (bCM), simulating consequent inflammatory responses, alone or combined. Compared to control cultures, spectrophotometric assays revealed shared treatment-dependent higher values of both calcium amounts and alkaline phosphatase activity for cultures involving the presence of elevated Pi. Ultrastructurally, shared peculiar pro-calcific degeneration patterns were exhibited by AVICs from these latter cultures irrespectively of the additional treatments. Disappearance of all cytomembranes and concurrent formation of material showing positivity to Cuprolinic Blue and co-localizing with silver precipitation were followed by the outcropping of such a material, which transformed in layers outlining the dead cells. Subsequent budding of these layers resulted in the formation of bubbling bodies and concentrically laminated calcospherulae mirroring those in actual soft tissue calcification. In conclusion, the *in vitro* models employed appear to be reliable tools for simulating metastatic calcification and indicate that hyperphosphatemic-like conditions could trigger valve calcification *per se*, with LPS and allogenic macrophage-derived secretory products acting as possible calcific enhancers *via* inflammatory responses. Anat Rec, 295:1117–1127, 2012. ©2012 Wiley Periodicals, Inc.

Key words: aortic valve calcification; metastatic calcification; inflammation; heart valve disease; valve interstitial cells

INTRODUCTION

Cardiovascular mortality still represents the leading cause of death in patients affected by end-stage renal disease. Derangement of divalent ion metabolism with consequent hyperphosphatemia, high calcium load, and increased calcium-phosphorus (Ca x P) product is suggested largely to contribute to the pathogenesis of valve

*Correspondence to: Fulvia Ortolani, Department of Experimental Clinical Medicine, University of Udine, Piazzale Kolbe 3, I-33100 Udine, Italy. E-mail: fulvia.ortolani@uniud.it

Received 30 November 2011; Accepted 29 March 2012.

DOI 10.1002/ar.22494

Published online 23 May 2012 in Wiley Online Library (wileyonlinelibrary.com).

calcification in uraemic patients (Ribeiro et al., 1998; Block, 2000; Tarrass et al., 2006). There is also increasing evidence suggesting that the mineralization of heart valves in dialysis patients shares multiple pathogenetic and clinical aspects with atherosclerosis including inflammation, lipid and lipoprotein deposition, and presence/regulation of bone-related proteins (Torun et al., 2005; Wang, 2009; Montasser et al., 2011).

In the attempt to clarify the mechanisms underlying cardiovascular tissue mineralization, in the last decade several *in vitro* models have been developed, providing a simulation of: (i) metastatic calcification, subjecting cells to high levels ($\geq$2 mmol/L) of either organic phosphate (Mathieu et al., 2005) or inorganic phosphate (Pi; Jono et al., 2000; Steitz et al., 2001; Giachelli et al., 2005); (ii) inflammation, treating cells with conditioned medium from cultures of heterogenic macrophages stimulated with bacterial endotoxin lipopolysaccharide (LPS; Tintut et al., 2002; Babu et al., 2008), which was supposed to contain pro-inflammatory cytokines, as recently confirmed (Xu et al., 2007; Wu et al., 2009); and (iii) co-existence of metastatic calcification and inflammation, stimulating cells cultured under mineralizing conditions with tumor necrosis factor alpha (TNF-α; Kaden et al., 2005) or LPS (Rattazzi et al., 2008).

Using these models, major results were that mineralization of cardiovascular tissues is associated with alkaline phosphatase (ALP) activity increasing as well as the expression of bone-related mediators in vascular smooth muscle cells or in aortic valve interstitial cells (AVICs), in contrast with other findings showing calcification of aortic valves to depend on various types of cell death processes (Kim, 1995; Jian et al., 2003; Somers et al., 2006; Rattazzi et al., 2008).

In previous studies on *in vivo* experimentally induced aortic valve mineralization, the calcific event was shown to depend on a peculiar AVIC degenerative process culminating with a lipid-release-dependent formation of peripheral phthalocyanin-positive layers (PPLs), acting as major hydroxyapatite (HA) nucleation sites at the level of cells and cell-derived vesicular bodies (Ortolani et al., 2002a,b, 2003, 2007). Similar calcific degenerative patterns were also found to take place in cultured AVICs using a novel *in vitro* model simulating dystrophic calcification (Ortolani et al., 2010).

In the present study, different *in vitro* conditions were accomplished to elucidate the possible contributes of putative agents in influencing metastatic calcification. Combined spectrophotometric estimations and ultrastructural analysis revealed how AVICs are responsive to the treatments, with elevated Pi alone a sufficient trigger of mineralization and possible enhancement exerted by LPS and species-specific pro-inflammatory mediators. In addition, calcification was found to correlate with a shared AVIC degeneration pattern as those described previously, which included the generation of final calcifying cell-derived structures superimposable to those existing in actual *in vivo* ectopic calcification.

MATERIALS AND METHODS

Isolation and Culture of Aortic Valve Interstitial Cells

Primary cultures of AVICs were obtained by enzymatic digestion of aortic valve leaflets isolated from hearts of slaughtered healthy bovines (age = 15 months), as previously described (Rattazzi et al., 2008). Namely, excised aortic roots were placed in Dulbecco's Modified Eagle's Medium (DMEM, Sigma) plus 1% penicillin/streptomycin and 1 μg/mL amphotericin B kept cool in ice. Then, aortic valve leaflets were isolated, depleted of endothelial cells by gentle surface scraping, and minced into $\sim$2–3 mm^3 pieces, which were digested with type-I collagenase (125 U/mL; Sigma), elastase (8 U/mL; Sigma), and soybean trypsin inhibitor (0.375 mg/mL; Sigma) for 30 min at 37°C. After digestion, the pieces were transferred into tissue culture Petri dishes (Greiner) and cultured in DMEM plus 20% Fetal Bovine Serum (FBS; Gibco), 1% L-glutamine, and 1% penicillin/streptomycin for 7–10 days. Once drawn from the digested pieces, AVICs were cultured in complete DMEM as above until pre-confluent state and expanded up to 10 folds. Cells from passages 4 to 6 were used. Light microscopy monitoring was made using an Olympus IX70 inverted microscope.

Conditioned Medium from Murine RAW264.7 Macrophages

Murine RAW264.7 macrophages were plated on tissue culture flasks (Falcon) and cultured in DMEM supplemented with 10% FBS, 1% L-glutamine, and 1% penicillin/streptomycin. At pre-confluence, RAW cells (passage 4) were stimulated with LPS (100 ng/mL; Sigma) for 1 hr at 37°C, rinsed twice with DMEM plus 10% FBS, and additionally cultured in complete DMEM for 12 hr achieving macrophage degranulation. After culture medium collection and centrifugation, supernatant was 0.22-μm-filtered, added with 1% polymyxin B (BioChemika) to neutralize residual LPS, and stored at −20°C until use.

Conditioned Medium from Bovine Fresh Macrophages

Fresh lympho/monocytes were collected by Ficoll® (1:2; Sigma) density gradient centrifugation of peripheral blood from healthy bovines (age = 18 months) before slaughtering and then plated on tissue culture flasks and maintained in complete DMEM, prepared as for RAW cells, overnight. After lymphocyte removing by rinsing with DMEM plus 10% FBS, monocytes were cultured in complete DMEM for 3 days to promote cell differentiation. These monocytes/macrophages were then treated like murine RAW264.7 macrophages.

AVIC Treatments

At pre-confluence, AVICs seeded on 35 mm culture plates (Greiner) were cultured in DMEM plus 10% FBS, 1% L-glutamine, and 1% penicillin/streptomycin (i) alone (control-cultures) or supplemented with: (ii) murine RAW264.7 macrophage conditioned medium equal to 1/5 of total supernatant volume (mCM-cultures); (iii) bovine macrophage conditioned medium equal to 1/5 of total supernatant volume (bCM-cultures); (iv) 100 ng/mL LPS (LPS-cultures); (v) 2.6 mM Pi (Pi-cultures); (vi) 2.6 mM Pi and 100 ng/mL LPS (Pi-LPS-cultures); (vii) 2.6 mM Pi, plus 100 ng/mL LPS, plus murine RAW264.7 macrophage conditioned medium equal to 1/5 of total supernatant volume (Pi-LPS-mCM-cultures); (viii) 2.6 mM Pi, plus 100 ng/mL LPS, plus bovine macrophage

conditioned medium equal to 1/5 of total supernatant volume (Pi-LPS-bCM-cultures). In each cell culture supplemented with 2.6 mM Pi, the final concentration of Pi was 3 mM. The treatments were performed for 3, 6, and 9 days, renewing the culture medium every 3 days.

Calcium Quantification

After culture medium recovering, cells were scraped from each culture plate, centrifuged, and treated with an aqueous lysis buffer containing 50 mM TRIS-HCl, 150 mM NaCl, 5 mM EDTA, and 1% Triton X-100, pH 7.4, for 1 hr at 4°C. After micro-centrifugation at 2000 rpm for 5 min, part of supernatant (500 μL) was recovered for ALP activity/protein assay and remaining lysed samples were rejoined to their original culture media and transferred into distinct Teflon vessels. Samples were added with 1 mL of 65% supra-pure grade nitric acid (Merck) and 500 μL of 30% supra-pure hydrogen peroxide (Merck), irradiated using the High Performance Microwave Digestion Unit mls 1200 mega (Milestone; 2 min at 250 W, 2 min at 0 W, 5 min at 300 W, 5 min at 450 W, and 6 min at 650 W), and diluted with ultra-pure water until obtaining 100 mL of total solution. Calcium quantification was assessed using the *o*-cresolphtalein complexone method (Chema Diagnostica) and absorbance was read at 575 nm with a Cary 50 Bio spectrophotometer (Varian). Each estimation came from 10 readings of five distinct experiments.

ALP Activity/Protein Assay

Supernatants (500 μL) obtained from micro-centrifugation of lysed samples were used to determine ALP activity and protein content. ALP activity was assessed using a kinetic method based on measurement of 4-nitrophenol production (Chema Diagnostica) reading the absorbance at 405 nm at 37°C within 5 min of enzymatic activity using the Cary 50 Bio spectrophotometer. Values corresponding to the trend line gradients coming from reading of five distinct experiments were normalized on the basis of protein content, estimated using a Coomassie Plus Protein Assay Reagent (Pierce) with absorbance reading at 595 nm using the spectrophotometer as above.

Ultrastructural Evidentiation of Polyanions with Pre-Embedding Reactions with Phthalocyanin Cuprolinic Blue

After culture medium removal, AVICs adhering to culture plates were washed twice with 0.1 M phosphate buffer and subjected to pre-embedding reaction with 0.05% phthalocyanin Cuprolinic Blue (CB; Electron Microscopy Sciences) dissolved in 25 mM sodium acetate buffer, containing 0.05 M magnesium chloride and 2.5% glutaraldehyde, pH 4.8, overnight, at room temperature and under continuous agitation. After further washing, AVICs were post-fixed with phosphate-buffered 2% osmium tetraoxide (Agar Scientific) for 1 hr at 4°C, washed again, dehydrated in graded ethanols, and embedded in Epon 812 resin. Thin sections were collected on formvar-coated 2 × 1-mm-slot copper grids and contrasted with uranyl acetate and lead citrate. Observations and photographic recordings were made using a Philips CM12/STEM electron microscope.

Ultrastructural Evidentiation of Calcium-Binding Sites with Post-Embedding Von Kossa Silver Staining

Semithin sections of CB-reacted and Epon-embedded AVICs were mounted on glass slides, covered with a drop of an aqueous solution of 1% silver nitrate, and placed on an 80°C warm plate under direct sunlight for 15 min. After washing with distilled water and drying, semithin sections were covered with a drop of an aqueous solution of 5% sodium thiosulfate at 80°C for 5 min for silver reduction. After further washing and drying, these semithin sections were re-embedded. Briefly, conic Beem capsules (Agar Scientific), previously cut at their top, were placed onto the slides encircling each reacted semithin section, glued at their base, and filled with Epon-Araldite fluid. After resin polymerization, the re-embedded sections underwent standard processing.

Statistical Analysis

The values of calcium amounts were reported as mean ± SD. Statistical differences among control and the different AVIC treatments were assessed using the ANOVA test, with Bonferroni correction for multiple comparisons. Values with $P < 0.0001$ were considered to be statistically significant.

RESULTS

To assess whether and how much elevated Pi and/or pro-inflammatory agents promote AVIC-mediated mineralization, spectrophotometric estimations of calcium amounts and ALP activity were carried out on treated primary cultures of cells derived from bovine aortic valve leaflets. ALP activity was tested because it is one of the most representative enzymes implicated in calcification.

In Fig. 1, the values are reported on the amounts of calcium contained in digested samples from AVIC cultures after 9-day-long treatments. The mean values resulted for samples from control-cultures, LPS-cultures, mCM-cultures, and bCM-cultures were similar to one another and collectively lower with respect to those in samples from the cultures supplemented with elevated Pi. Also, these higher mean values were similar to one another, except for the Pi-LPS-bCM-cultures, which contained even more mineral.

The values of ALP activity in the 9-day-long AVIC cultures are reported in Fig. 2. Compared to control-cultures, no change resulted for mCM-cultures and bCM-cultures, a weak increase for LPS-cultures, and a further weak increase for Pi-cultures. A marked increase resulted for the remaining cultures, being the highest value measured for Pi-LPS-cultures, with linearly lower values for Pi-LPS-mCM-cultures and Pi-LPS-bCM-cultures, respectively.

Since the values of calcium content were markedly increased for all four cultures containing elevated Pi, whereas higher ALP activity only resulted for the cultures containing elevated Pi combined with other treatments but not Pi alone, supplementary estimations of this parameter were supplied for all these cultures verifying the time course spanning 3–9 days (Fig. 3). In detail, enzymatic activity reached a maximum at 6-day-

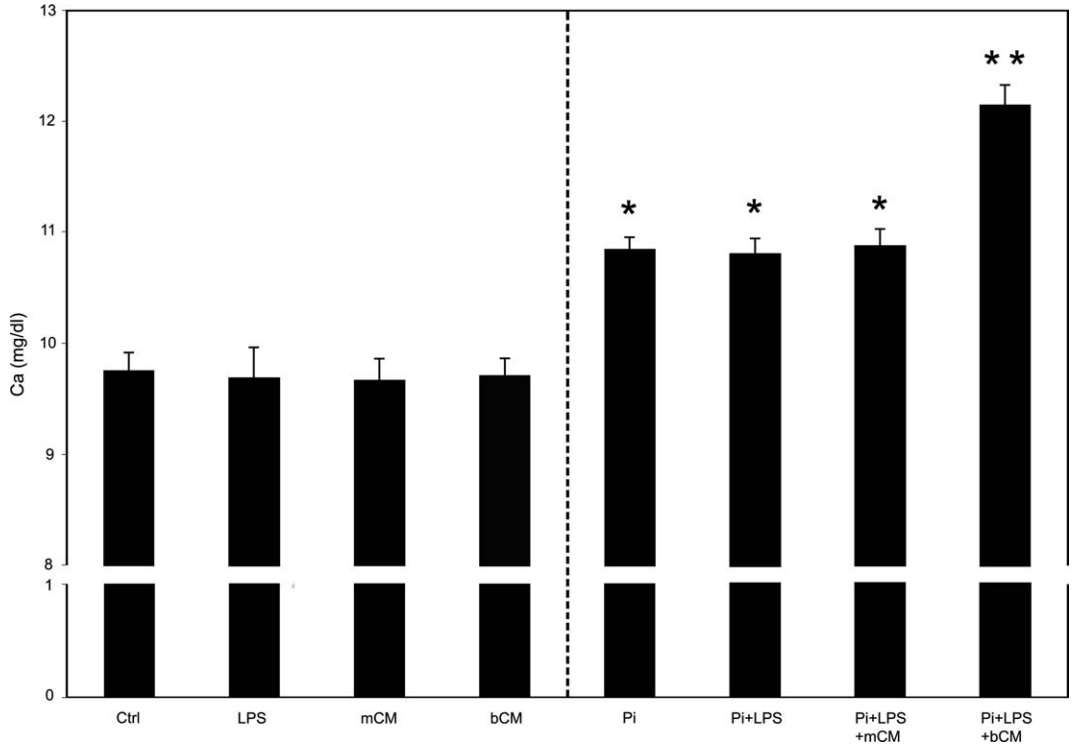

Fig. 1. Spectrophotometric estimation of calcium amounts for 9-day-long-cultured bovine AVICs with no treatment (Ctrl) or after different stimuli alone or combined, that is, lipopolysaccharide (LPS), murine conditioned medium (mCM), bovine conditioned medium (bCM), and elevated (2.6 mM) inorganic phosphate (Pi), with the vertical hatched line distinguishing Pi-lacking treatments from Pi-containing ones. The values are reported as mean ± SD. The values concerning the treated cultures are significantly different (*) from those of control-cultures, and those concerning Pi-LPS-bCM-cultures are significantly different (**) from all others; $P < 0.0001$.

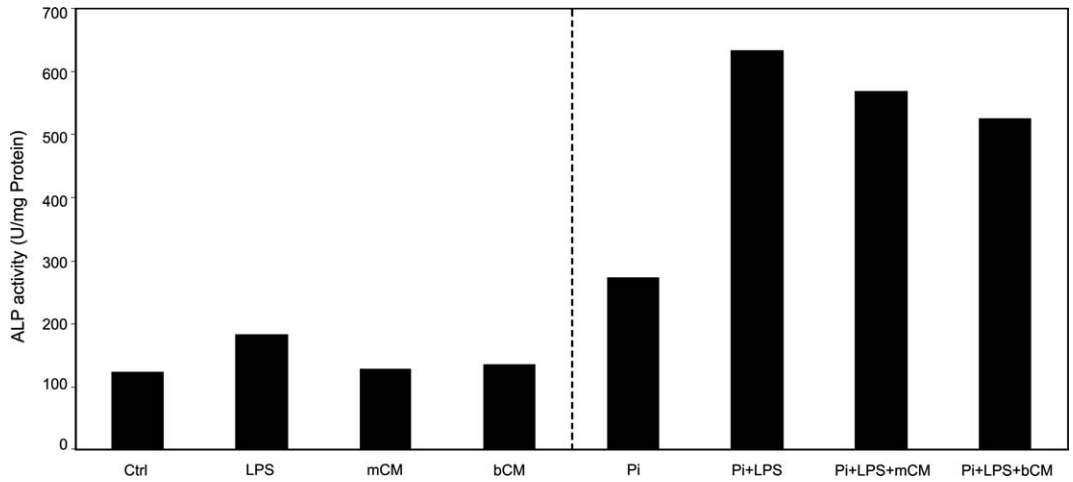

Fig. 2. Spectrophotometric estimation of ALP activity for 9-day-long-cultured bovine AVICs with no treatment or after the different stimulations as in Fig. 1.

long incubation for Pi-cultures, with a subsequent drop at 9 days. Conversely, enzymatic activity underwent a roughly linear increase up to day 9 for Pi-LPS-, Pi-LPS-mCM-, and Pi-LPS-bCM-cultures.

Morphologically, the mineralization rates induced by the applied treatments were readily recognizable under the inverted microscope on the basis of size and number of formed calcific nodules. The presence of calcific nodules only in Pi-containing cultures was apparent as well as the most marked calcification occurring in Pi-LPS-bCM cultures (Fig. 4).

Severity of cell alterations was assessed at the ultrastructural level on samples subjected to pre-embedding histochemical reactions based on the use of acidic

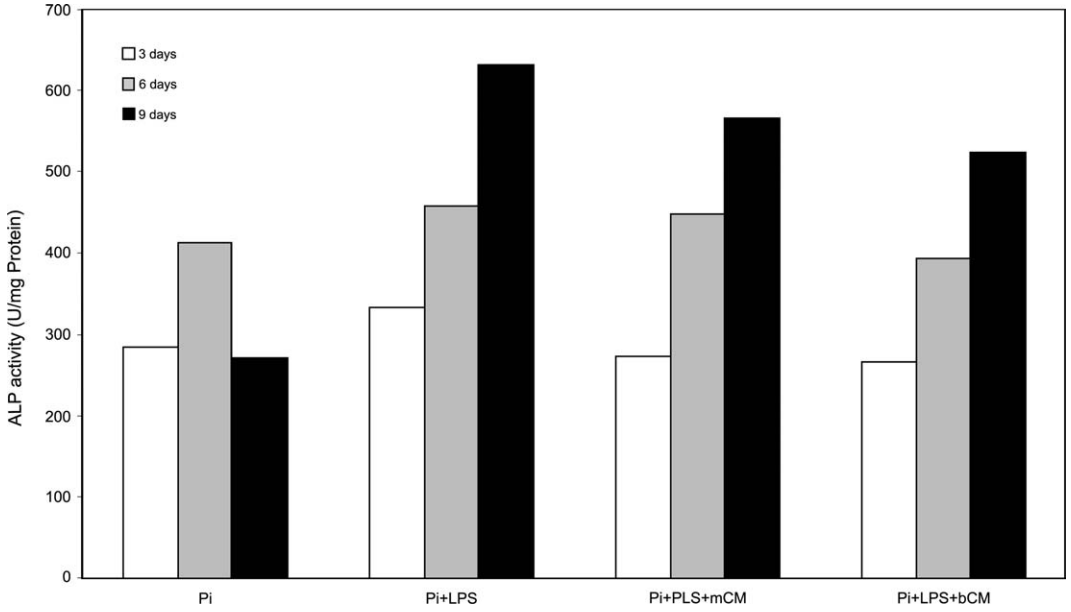

Fig. 3. Spectrophotometric estimation of ALP activity time course spanning 3–9 days for bovine AVIC cultures after all treatments involving the presence of elevated Pi.

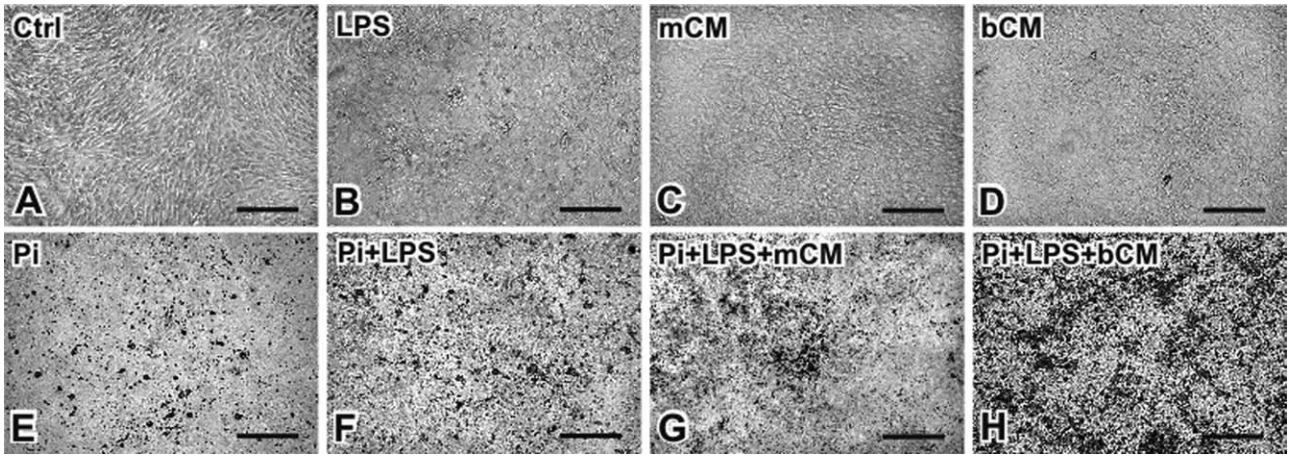

Fig. 4. Light microscopy micrographs of unstained AVIC monolayers. **A–D:** Absence of calcium precipitation in control cultures (Ctrl) and cultures treated with lipopolysaccharide alone (LPS), murine derived conditioned medium alone (mCM), and bovine derived conditioned medium alone (bCM). **E–H:** Presence of calcium precipitation in monolayer cultures treated with elevated (2.6 mM) inorganic phosphate alone (Pi), Pi+LPS, Pi+LPS+mCM, and Pi+LPS+bCM. Original magnification: 10×.

mixtures of glutaraldehyde and copper phthalocyanin Cuprolinic Blue (CB; see Materials and Methods session). Since this mixture allows sample decalcification with simultaneous retention of acidic-lipid-containing material resulting from the degradation of cytoplasmic organules and membranes, this method previously showed the peculiarity of the AVIC degeneration occurring in *in vivo* experimental models of accelerated calcification (Ortolani et al., 2002a,b, 2003, 2007) as well as in an *in vitro* model simulating dystrophic calcification (Ortolani et al., 2010). In addition, resin semithin sections of CB-reacted samples were subjected to post-embedding reactions based on metallic silver precipitation, namely the reaction of von Kossa, widely used on histological sections to detect calcific sites (see Materials and Methods session).

On thin sections, control AVICs showed well preserved intracytoplasmic organelles and lamellipodia with associated anchoring stress fibers (Fig. 5A,B), that is, the flat protoplasmic protrusions and cytoskeleton filaments which usually characterize adhering cultured cells.

As in controls, no apparent damage was appreciable for AVICs from mCM-cultures, bCM-cultures, and LPS-cultures (not shown). In all experiments in which elevated Pi was present, a distinct cell degenerative process was observed which included (i) degeneration of cytoplasmic organules, (ii) release of CB-reactive material, and (iii) margination of this material and its outward budding. In

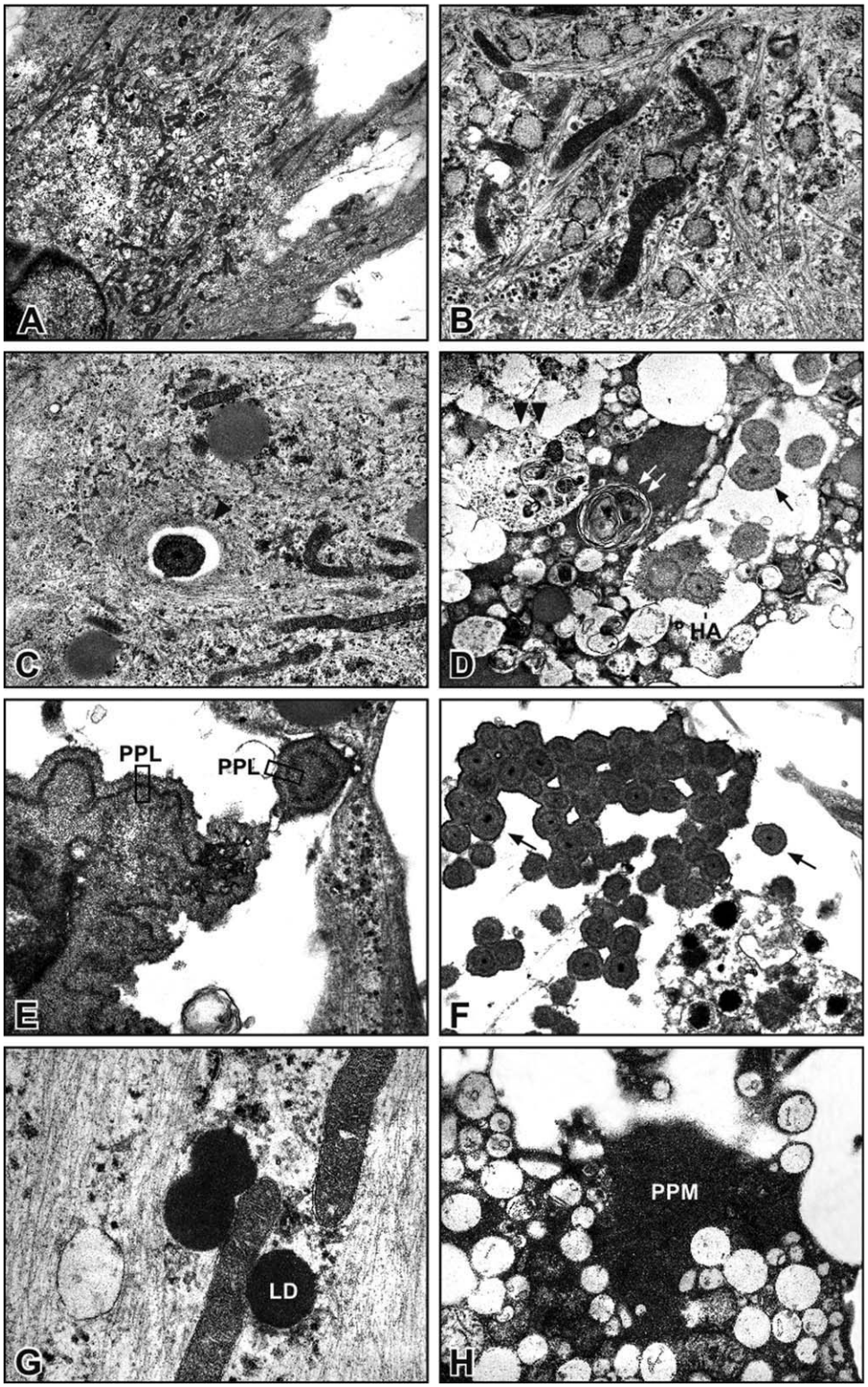

Fig. 5. **A** and **B:** Thin sections showing normal features in AVICs from control-cultures. **C–F:** Altered features in AVICs from cultures added with 2.6 mM Pi: autophagocytic vacuole (double arrowhead in D); myelin figure (double white arrow in D); CB-reactive layers (frame-PPL in E); calcospherulae (black arrows in D and F); phagocyted calcospherula (arrowhead in C); hydroxyapatite crystals (HA in D). **G:** CB-reactive lipid droplets (LD) in an AVIC cultured with Pi+LPS. **H:** Vesiculation and CB-reactive material (PPM) in an AVIC cultured with Pi+LPS+mCM. Magnifications: 3,000× (A); 12,000× (B); 9,000× (C and D); 20,000× (E); 7,000× (F); 25,000× (G); 11,000× (H).

more detail, initial AVIC alteration consisted in the abnormous dilation of rough endoplasmic reticulum, swelling of mitochondria with progressive dissolution of christae, cytoplasm vesiculation, mounting disruption/loss of all membrane-bound organelles and nuclear envelope, with the appearance of a lot of phthalocyanin-reactive lipid droplets, autophagocytic vacuoles/lysosomes, and myelin figures (Figs. 5D,G,H and 6A,C,D). Cytoplasm vacuolization also depended on depletion of swollen mitochondria and was complicated by their joining/fusion into greater vacuoles. During these processes, previously accumulated lipid-like amorphous material was poured into the major vacuoles, transforming them into lipid inclusions subsequent to fragmentation and dissolution of lining membranes (Figs. 5H and 6C). The resulting lipid inclusions underwent a progressive increase in reactivity to pre-embedding reaction with CB (Figs. 5G and 6A) and were selective sites for metallic silver particle deposition, after additional post-embedding von Kossa silver staining (Fig. 6B). An incipient increase in cytoplasm electrondensity seemed to result from the melting of these reactive lipid droplets with associated overgrowing of amorphous phthalocyanin-positive material (PPM), which entrapped organule-derived remnants and clusters of degrading ribosomes (Figs. 5H and 6D).

More advanced degenerative features were (i) shortening/disappearance of lamellipodia, with cells acquiring smoothed profiles and irregularly roundish shapes, (ii) complete colliquation of organules, and (iii) their replacement by increasing PPM. Centrifugal PPM spreading in waves followed, resulting in the appearance of multilaminated, CB-reactive PPLs outlining the body of cell remnants and being 100–200 nm thick (Figs. 5E and 6E). Initial pseudo-orthogonal precipitation of needle-like HA crystals appeared mostly to occur at level of PPLs, revealing their marked pro-calcific role (Fig. 6F). The same involvement was exhibited by initial PPL-derived bodies, detaching from cell surface and, to a lesser extent, intracellular transitional forms of PPM into PPLs. Co-localization between HA crystal nucleation and metallic silver precipitation was also evident after von Kossa reactions (Fig. 6G).

These degenerative phenomena appeared to end with the dead PPL-lined cells undergoing fragmentation into heterogeneously sized bubbling bodies (Fig. 7A,B), with overlapping sporulation-like PPL budding and pinching off, so generating rounded concentrically laminated calcospherulae mostly characterized by a punctate dense core, with diameters ranging between 130 nm and 1 μm (Fig. 7A–E). Also these PPL-derivatives were strongly reactive to silver von Kossa reactions (Fig. 7F).

It is worth noting that stimulation with elevated Pi alone was sufficient to give rise to all degenerative patterns including the genesis of calcospherulae (Fig. 5D). Of interest, calcospherulae phagocytated by still viable AVICs were encountered (Fig. 5C).

DISCUSSION

The elevated Pi concentration settled in the AVIC cultures was consistent with the hyperphosphatemic conditions in organisms, thus allowing to test the implications of this inorganic element, as well as bacterial endotoxin LPS and macrophage-derived inflammatory mediators, in a context reproducing metastatic calcification.

Aside from the additional stimulations, prominent calcific events occurred in all cultures containing elevated Pi. Since Pi concentration (3 mM) was consistent with conditions of severe hyperphosphatemia, such a condition seems to be capable of inducing ectopic calcification *per se*, consistently with the concept that elevated Ca x P product represents the most predictive parameter for cardiac valve calcification in hemodialysis patients (Ribeiro et al., 1998; Block, 2000; Tarrass et al., 2006).

Compared to Pi-cultures, additional increase in calcium amount resulted for Pi-LPS-bCM cultures exclusively. The absence of increase in calcium amounts after superstimulation of 9-day-cultured AVICs with endotoxin LPS is not consistent with a previous report of marked mineralization occurring in Pi-LPS treated AVIC cultures (Rattazzi et al., 2008). However, those results concerned longer incubation times. On the other hand, the highest ALP activity resulted for Pi-LPS treatment in the present investigation. Of note, direct pro-calcific effects by LPS, including ALP activity enhancement, were shown to occur for cultured AVICs with the involvement of specific LPS Toll-like receptors (TLRs; Babu et al., 2008; Meng et al., 2008; Yang et al., 2009). Thus, it seems likely that this bacterial endotoxin can exert some pro-calcific effect on AVICs, superimposing to that exerted by elevated Pi.

Additional stimulations with conditioned media derived from cultures of monocytes/macrophages, in their turn stimulated with LPS, were accomplished with the rationale of simulating inflammatory conditions due to a bacterial infection in the organism. A stimulation with conditioned medium from LPS-stimulated monocytes/macrophages was already used on a subset of bovine aorta-wall-derived smooth muscle cells (Tintut et al., 2002), named calcific vascular cells (CVCs; Watson et al., 1994), eliciting TNF-α secretion associated with increased ALP activity. Moreover, specific interaction of LPS with TLR-4 was reported to prime the activation of murine RAW264.7 macrophages, suggesting their contribution in mineralizing processes (Hume et al., 2001; Wu et al., 2009).

In this investigation, conditioned media from cultures of LPS-activated RAW264.7 macrophages did not cause increase in mineralization, whereas a clear calcific outgrowth occurred by using conditioned media from cultures of allogenic primary macrophages. Taking into account that macrophage activation by bacterial wall components correlates with secretion of species-specific chemo/cytokines (Nagao et al., 1992) and that equal pathogen doses can trigger different inflammatory cell responses (Munford, 2010; Warren et al., 2010), it is feasible that species-specific macrophage-derived cytokines are needed to enhance calcific responses by AVICs.

Together, the above results are in line with the concept that products derived from GRAM-negative bacteria may contribute in triggering cardiac valve calcification *via* inflammatory reactions, as suggested by the detection of Chlamydia pneumoniae in both stenotic and sclerotic semilunar valves (Juvonen et al., 1997; Nyström-Rosander et al., 1997), as well as the experimental demonstration that animal aortic valves undergo mineralizing effects after inoculation with oral bacteria (Cohen et al., 2004).

Concerning ALP activity in 9-day-long cultures, prominent increases were restricted to the three cultures

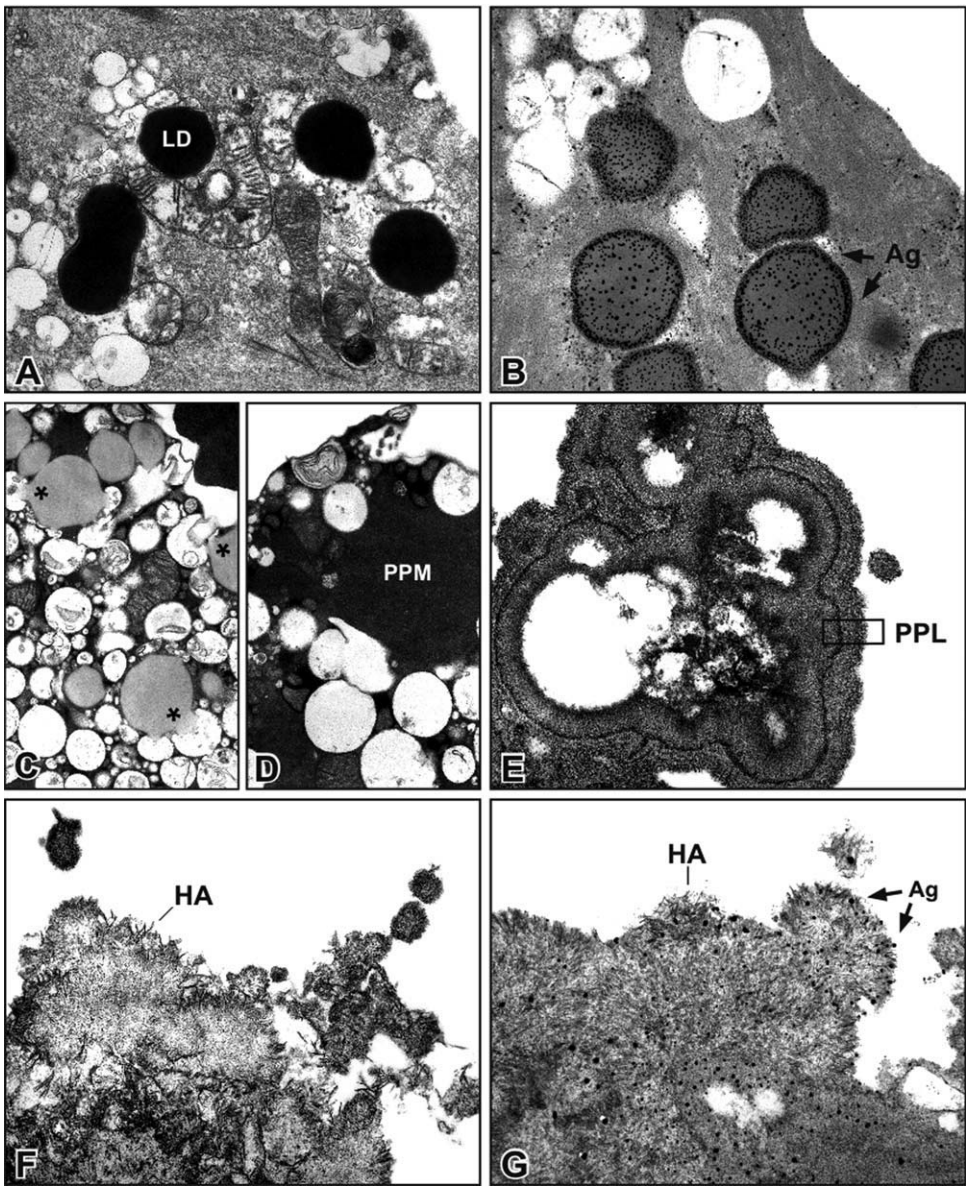

Fig. 6. **A–G:** Thin sections showing altered features in AVICs from cultures added with 2.6 mM-Pi+LPS+bCM: CB-reactive lipid droplets (LD in A); selective precipitation of metallic silver (Ag with arrows in B and G); vesiculation (in C and D) with inter-vesicule lipid material pouring (asterisks in C); CB-reactive material (PPM in D); CB-reactive multi-laminated layer (frame-PPL in E); hydroxyapatite crystals (HA in F and G). Magnifications: 14,000× (A); 20,000× (B); 11,000× (C); 13,000× (D); 17,000× (E and F); 25,000× (G).

subjected to superstimulation with LPS and LPS plus conditioned media. Since prominent increase in calcium amount was a response shared by Pi-cultures and all superstimulated cultures, analogous sharing was expected to exist for ALP activity. This was not the case because of lower enzyme activity for Pi-cultures. On extending the estimation of ALP activity to 3-day and 6-day long cultures, a similar increase was shared by all four culture types up to 6 incubation days, whereas there was a marked drop in Pi-cultures between the sixth and the ninth day, in contrast with a further increase occurring for the other three treatments. This was consistent with the reported finding of lower activity for AVIC Pi-cultures *versus* Pi-LPS cultures (Rattazzi et al., 2008). Thus, it is reasonable that ALP activity may be involved in mineralization but without acting as an exclusive driving factor.

Of interest, pro-inflammatory cytokines such as TNF-α were reported to induce over-expression of type III sodium-dependent Pi cotransporter PiT-1 (Li and Giachelli, 2007), with a possible increase in Pi uptake by cultured mineralizing vascular smooth muscle cells (Lau et al., 2010). Putatively, a differential cytokine-induced over-expression of PiT-1 by AVICs and consequent massive Pi uptake might enhance calcium phosphate formation, thereby eliciting greater HA precipitation at the edges of AVICs and AVIC-derived products in Pi-LPS-bCM cultures, independently from the rate of ALP activity.

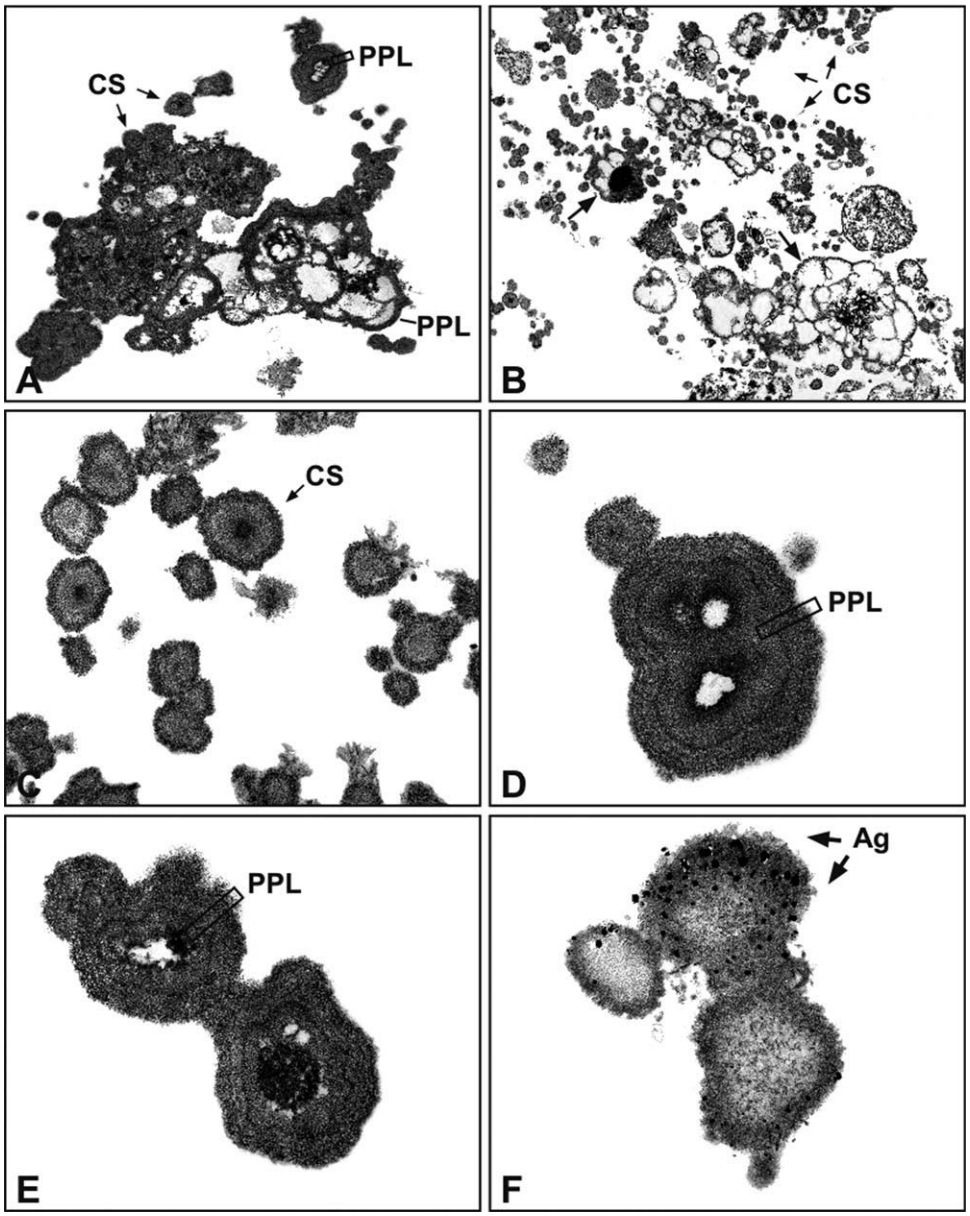

Fig. 7. **A–F:** Thin sections showing cell-derived products subsequent to fragmentation of AVICs from cultures added with 2.6 mM-Pi+LPS+bCM: concentrically laminated calcospherulae (CS with arrows in A–C); bubbling bodies (single arrows in B); and minor fragments showing CB-reactive layers (frame-PPL in A, D, and E); selective precipitation of metallic silver (Ag with arrows in F). Magnifications: 4,000× (A and B); 21,000× (C); 25,000× (D); 23,000× (E and F).

It is worth to note that increases in ALP activity were never associated with signs suggesting some AVIC trans-differentiation into osteoblast-like cells, being the progression of calcific processes exclusively accompanied by advancing of the described pro-calcific degenerative patterns showed by the dying/died cultured AVICs.

Although apoptosis was reported to occur for cultured ovine calcifying AVICs stimulated with transforming growth factor beta (TGF-β; Jian et al., 2003) as well as a specific clone of bovine AVICs after stimulation with LPS (Rattazzi et al., 2008), neither ultrastructural hallmarks nor positivity to TUNEL tests (not presented) were found in the present investigation. Rather, the observation of frequent macroautophagocytosis figures at the early treatment stages might suggest that autophagic cell death might be primed, as reported for calcified aortic valve stenosis (Somers et al., 2006), with the occurrence of unusually extensive lipolytic processes, possibly resulting in a prominent release of phospholipids and free fatty acids, consistently with the observed reactivity to cationic dye CB. Work is in progress to ascertain whether the observed degeneration patterns depend on a sudden unregulated cell breakdown or are the final steps of an aborted orthodox type of cell death, if not of a wholly undescribed type of regulated cell death.

Size and number of calcific nodules observed with light inverted microscope for Pi-containing cultures were morphological parameters fitting with the treatment-dependent increases in calcium amount spectrophotometrically estimated. Consistently, ultrastructural analysis clearly indicated that all treated AVICs underwent dramatic breakdown including intracellular release/accumulation of CB-reactive and silver-reactive material as well as its outcropping with formation of the pericellular dark layers named PPLs. A similar cell degradation process was already described for experimental *in vivo* calcification consisting in xenogenic subdermal implantation of glutaraldehyde-treated aortic valve cusps, with PPLs resulting to be largely formed by lipidic moieties including phospholipids and to contain calcium-binding sites (Ortolani et al., 2002a,b, 2003, 2007), as well as experimental *in vitro* models of ectopic calcification (Ortolani et al., 2010). Additionally, ultrastructural features reminiscent of PPLs were described for calcific aortic valves and other soft tissues affected by ectopic calcification as alcianophylic envelopes outlining so called "thick walled cell derived products" (CDPs; Kim and Huang, 1971; Kim, 1976; Boskey et al., 1988; Kim, 1995).

Since PPM production paralleled a progressive disappearance of all cytomembrane-bounded organelles, derived membranous residues and nuclear chromatin, it ensues that such a substance results from a complete colliquation of all these components. This was also confirmed by the observation of a lot of transitional patterns showing disrupting organelles or their ghosts to merge with PPM or to be embedded within such a material.

The role of these cell-derived products as major HA nucleators was supported by co-localization of calcium-binding sites, as revealed by the selective precipitation of metallic silver after von Kossa staining, as well as effective superimposition of HA crystals.

A further significant outcome in the present study was the identification of multilayered PPLs and concentrically laminated calcospherulae, these latter being closely reminiscent of the typical "porous particles in concentric layering" described for calcific aortic valves and other tissues affected by ectopic calcification (Kim, 1995) as well as failed calcific valve bioprostheses (Valente et al., 1985).

Because of affinity to von Kossa silver staining and superimposition by HA crystals, the calcospherulae seem to act as mineralization enhancers in the most advanced calcific stages, providing a widespread dissemination of supernumerary nucleation sites. This role is analogous to that played by matrix vesicles and/or apoptotic bodies in both physiological calcification and pathological one (Anderson, 1983; Kirsch, 2006), although being quite different cell-derived structures. In fact, calcospherulae appeared to result from a passive budding of PPLs and lack in cytoplasm, showing a roughly shared para-crystalline structure because of the presumable rearrangement of the pre-existent array of the lipid moiety at the level of the PPL-forming layers. Conversely, matrix vesicles and apoptotic bodies are described to result from distinct regulated mechanisms, contain organized cytoplasm, and are outlined by membranes with specific molecular architectures, including either inner location of phospholipids (Wu et al., 1997) or outer location (Bratton et al., 1997), respectively.

In conclusion, the used *in vitro* models represent reliable tools for simulating metastatic heart valve calcification, being calcospherulae actual structures characterizing ectopic mineralization, and the obtained results suggest that metastatic calcification in systemic conditions results from a peculiar AVIC degeneration and subsequent death which is triggered by hyperphosphatemia *per se*, with possible enhancing effects exerted by bacterial products and pro-inflammatory mediators.

LITERATURE CITED

Anderson HC. 1983. Calcific diseases: a concept. Arch Pathol Lab Med 107:341–348.

Babu AN, Meng X, Zou N, Yang X, Wang M, Song Y, Cleveland JC, Weyant M, Banerjee A, Fullerton DA. 2008. Lipopolysaccharide stimulation of human aortic valve interstitial cells activates inflammation and osteogenesis. Ann Thorac Surg 86:71–76.

Block GA. 2000. Prevalence and clinical consequences of elevated Ca x P product in hemodialysis patients. Clin Nephrol 54:318–324.

Boskey AL, Bullough PG, Vigorita V, Di Carlo E. 1988. Calcium-acidic phospholipid-phosphate complexes in human hydroxyapatite-containing pathologic deposits. Am J Pathol 133:22–29.

Bratton DL, Fadok VA, Richter DA, Kailey JM, Guthrie LA, Henson PM. 1997. Appearance of phosphatidylserine on apoptotic cells requires calcium-mediated nonspecific flip-flop and is enhanced by loss of the aminophospholipid translocase. J Biol Chem 272:26159–26165.

Cohen DJ, Malave D, Ghidoni JJ, Iakovidis P, Everett MM, You S, Liu Y, Boyan BD. 2004. Role of oral bacterial flora in calcific aortic stenosis: an animal model. Ann Thorac Surg 77:537–543.

Giachelli CM, Speer MY, Li X, Rajachar RM, Yang H. 2005. Regulation of vascular calcification: roles of phosphate and osteopontin. Circ Res 96:717–722.

Jian B, Narula N, Li QY, Mohler ER, III, Levy RJ. 2003. Progression of aortic valve stenosis: TGF-beta1 is present in calcified aortic valve cusps and promotes aortic valve interstitial cell calcification *via* apoptosis. Ann Thorac Surg 75:457–466.

Jono S, McKee MD, Murry CE, Shioi A, Nishizawa Y, Mori K, Morii H, Giachelli CM. 2000. Phosphate regulation of vascular smooth muscle cell calcification. Circ Res 87:e10–e17.

Juvonen J, Laurila A, Juvonen T, Aläkarppä H, Surcel HM, Lounatmaa K, Kuusisto J, Saikku P. 1997. Detection of Chlamydia pneumoniae in human nonrheumatic stenotic aortic valves. J Am Coll Cardiol 29:1054–1059.

Hume DA, Underhill DM, Sweet MJ, Ozinsky AO, Liew FY, Aderem A. 2001. Macrophages exposed continuously to lipopolysaccharide and other agonists that act *via* toll-like receptors exhibit a sustained and additive activation state. BMC Immunol 2:11.

Kaden JJ, Kiliç R, Sarikoç A, Hagl S, Lang S, Hoffmann U, Brueckmann M, Borggrete M. 2005. Tumor necrosis factor alpha promotes an osteoblast-like phenotype in human aortic valve myofibroblasts: a potential regulatory mechanism of valvular calcification. Int J Mol Med 16:869–872.

Kim KM. 1976. Calcification of matrix vesicles in human aortic valve and aortic media. Federation Proc 35:156–162.

Kim KM. 1995. Apoptosis and calcification. Scanning Microsc 9: 1137–1178.

Kim KM, Huang S. 1971. Ultrastructural study of calcification of human aortic valve. Lab Invest 25:357–366.

Kirsch T. 2006. Determinants of pathological mineralization. Curr Opin Rheumatol 18:174–180.

Lau WL, Festing MH, Giachelli CM. 2010. Phosphate and vascular calcification: emerging role of the sodium-dependent phosphate cotransporter PiT-1. Thromb Haemost 104:464–470.

Li X, Giachelli CM. 2007. Sodium-dependent phosphate cotransporters and vascular calcification. Curr Opin Nephrol Hypertens 16: 325–328.

Mathieu P, Voisine P, Pépin A, Shetty R, Savard N, Dagenais F. 2005. Calcification of human valve interstitial cells is dependent on alkaline phosphatase activity. J Heart Valve Dis 14:353–357.

Meng X, Ao L, Song Y, Babu A, Yang X, Wang M, Weyant MJ, Dinarello CA, Cleveland JC, Jr, Fullerton DA. 2008. Expression

of functional Toll-like receptors 2 and 4 in human aortic valve interstitial cells: potential roles in aortic valve inflammation and stenosis. Am J Physiol Cell Physiol 294:C29–C35.

Montasser D, Bahadi A, Zajjari J, Asserraji M, Aloyoude A, Moujoud O, Aattif T, Kadiri M, Zemraoui N, El Kabbaj D, Hassani M, Benyahia M, El Allam M, Oualim Z, Akhmouch I. 2011. Infective endocarditis in chronic hemodialysis patients: experience from Morocco. Saudi J Kidney Dis Transpl 22:160–166.

Munford RS. 2010. Murine responses to endotoxin: another dirty little secret? J Infect Dis 201:175–177.

Nagao S, Akagawa KS, Okada F, Harada Y, Yagawa K, Kato K, Tanigawa Y. 1992. Species dependency of *in vitro* macrophage activation by bacterial peptidoglycans. Microbiol Immunol 36: 1155–1171.

Nyström-Rosander C, Thelin S, Hjelm E, Lindquist O, Pahlson C, Friman G. 1997. High incidence of Chlamydia pneumoniae in sclerotic heart valves of patients undergoing aortic valve replacement. Scand J Infect Dis 29:361–365.

Ortolani F, Bonetti A, Tubaro F, Petrelli L, Contin M, Nori SL, Spina M, Marchini M. 2007. Ultrastructural characterization of calcification onset and progression in subdermally implanted aortic valves. Histochemical and spectrometric data. Histol Histopathol 22:261–272.

Ortolani F, Petrelli L, Tubaro F, Spina M, Marchini M. 2002a. Novel ultrastructural features as revealed by phthalocyanin reactions indicate cell priming for calcification in subdermally implanted aortic valves. Connect Tissue Res 43:44–55.

Ortolani F, Petrelli L, Nori SL, Spina M, Marchini M. 2003. Malachite green and phthalocyanin-silver reactions reveal acidic phospholipid involvement in calcification of porcine aortic valves in rat subdermal model. Histol Histopathol 18:1131–1140.

Ortolani F, Rigonat L, Bonetti A, Contin M, Tubaro F, Rattazzi M, Marchini M. 2010. Pro-calcific responses by aortic valve interstitial cells in a novel *in vitro* model simulating dystrophic calcification. Ital J Anat Embryol 115:135–139.

Ortolani F, Tubaro F, Petrelli L, Gandaglia A, Spina M, Marchini M. 2002b. Specific relation between mineralization and cuprolinic blue uptake as revealed by copper retention in calcified aortic valves and ultrastructural evidences. Histochem J 34:41–50.

Rattazzi M, Iop L, Faggin E, Bertacco E, Zoppellaro G, Baesso I, Puato M, Torregrossa G, Fadini GP, Agostini C, Gerosa G, Sartore S, Pauletto P. 2008. Clones of interstitial cells from bovine aortic valve exhibit different calcifying potential when exposed to endotoxin and phosphate. Arterioscler Thromb Vasc Biol 28:2165–2172.

Ribeiro S, Ramos A, Brandão A, Rebelo JR, Guerra A, Resina C, Vila-Lobos A, Carvalho F, Remédio F, Ribeiro F. 1998. Cardiac valve calcification in haemodyalisis patients. Role of calcium-phosphate metabolism. Nephrol Dial Transplant 13:2037–2040.

Somers P, Knaapen M, Kockx M, van Cauwelaert P, Bortier H, Mistiaen W. 2006. Histological evaluation of autophagic cell death in calcified aortic valve stenosis. J Heart Valve Dis 15:43–48.

Steitz SA, Speer MY, Curinga G, Yang HY, Haynes P, Aebersold R, Schinke T, Karsenty G, Giachelli CM. 2001. Smooth muscle cell phenotypic transition associated with calcification: upregulation of Cbfa1 and downregulation of smooth muscle lineage markers. Circ Res 89:1147–1154.

Tarrass F, Benjelloun M, Zamd M, Medkouri G, Hachim K, Benghanem MG, Ramdani B. 2006. Heart valve calcifications in patients with end-stage renal disease: analysis for risk factors. Nephrology 11:494–496.

Tintut Y, Patel J, Territo M, Saini T, Parhami F, Demer LL. 2002. Monocyte/macrophage regulation of vascular calcification *in vitro*. Circulation 105:650–655.

Torun D, Sezer S, Baltali M, Adam FU, Erdem A, Ozdemir FN, Haberal M. 2005. Association of cardiac valve calcification and inflammation in patients on hemodialysis. Ren Fail 27:221–226.

Valente M, Bortolotti U, Thiene G. 1985. Ultrastructural substrates of dystrophic calcification in porcine bioprosthetic valve failure. Am J Pathol 119:12–21.

Wang AYM. 2009. Vascular and other tissue calcification in peritoneal dialysis patients. Perit Dial Int 29:S9–S14.

Warren HS, Fitting C, Hoff E, Adib-Conquy M, Beasley-Topliffe L, Tesini B, Liang X, Valentine C, Hellman J, Hayden D, Cavaillon JM. 2010. Resilience of bacterial infection: difference between species could be due to proteins in serum. J Infect Dis 201:223–232.

Watson KE, Boström K, Ravindranath R, Lam T, Norton B, Demer LL. 1994. TGF-beta 1 and 25-hydroxycholesterol stimulate osteoblast-like vascular cells to calcify. J Clin Invest 93:2106–2113.

Wu LN, Genge BR, Dunkelberger DG, LeGeros RZ, Concannon B, Wuthier RE. 1997. Physicochemical characterization of the nucleational core of matrix vesicles. J Biol Chem 272:4404–4411.

Wu TT, Chen TL, Chen RM. 2009. Lipopolysaccharide triggers macrophage activation of inflammatory cytokine expression, chemotaxis, phagocytosis, and oxidative ability *via* a toll-like receptor 4-dependent pathway: validated by RNA interference. Toxicol Lett 191:195–202.

Xu Z, Huang CX, Li Y, Wang PZ, Ren GL, Chen CS, Shang FJ, Zhang Y, Liu QQ, Jia ZS, Nie QH, Sun YT, Bai XF. 2007. Toll-like receptor 4 siRNA attenuates LPS-induced secretion of inflammatory cytokines and chemokines by macrophages. J Infect 55: e1–e9.

Yang X, Fullerton DA, Su X, Ao L, Cleveland JC, Jr, Meng X. 2009. Pro-osteogenic phenotype of human aortic valve interstitial cells is associated with higher levels of Toll-like receptors 2 and 4 and enhanced expression of bone morphogenetic protein 2. J Am Coll Cardiol 53:491–500.